

Grain-boundary dissociation by the emission of stacking faults

J. D. Rittner and D. N. Seidman

Department of Materials Science and Engineering and the Materials Research Center, R. R. McCormick School of Engineering and Applied Science, Northwestern University, Evanston, Illinois 60208

K. L. Merkle

Materials Science Division, Argonne National Laboratory, Argonne, Illinois 60439

(Received 2 October 1995)

A range of $\langle 110 \rangle$ symmetric tilt grain boundaries (GB's) are investigated in several fcc metals with simulations and high-resolution electron microscopy. Boundaries with tilt angles between 50.5° and 109.5° dissociate into two boundaries 0.6 to 1.1 nm apart. The dissociation takes place by the emission of stacking faults from one boundary that are terminated by Shockley partials at a second boundary. This is a general mode of GB relaxation for low stacking fault energy metals. The reasons for the occurrence of this relaxation mode are discussed using the theory of GB dislocations.

Most high-angle grain boundaries (GB's) are observed to have narrow structures with the atomic relaxations extending only a few angstroms into either grain. Recently, observations¹ have been made of GB's with wider structures—up to a nanometer or more in width. Wide GB structures had been found earlier, although they were not recognized as such, in both high-resolution electron microscopy of gold boundaries² and simulations of copper boundaries.³ These wide GB's have also been called three-dimensional boundaries. In many cases, wide GB structures are the result of emission of stacking faults from the boundary into one or both grains. The stacking faults terminate in partial dislocations that create a low-angle GB. Thus, the original GB dissociates into two or even three GB's by emitting stacking faults. We present evidence from computer simulations and high-resolution electron microscopy (HREM) experiments that this mode of relaxation occurs frequently for $\langle 110 \rangle$ tilt GB's in fcc metals and is not unique to specific boundaries. A range of symmetry $[1\bar{1}0]$ tilt GB's with tilt angles between $\theta=50.48^\circ$ and 109.47° are investigated in several fcc metals.

Computer simulations using the lattice statics technique are performed on eight GB's using embedded-atom-method⁴ (EAM) potentials for Al,⁵ Au, and Ni.⁶ The area of the boundary planes in the computational cells ranges from 71 to 99 nm² and the cells contain a total of 6528–8448 atoms. The periodic borders parallel to the boundary plane are permitted to move, thus allowing constant zero pressure simulations. The periodic borders perpendicular to the boundary plane are held fixed at lengths determined from the equilibrium lattice constant to counteract the GB tension. Rigid-body translations between the two crystals are allowed and are used to create from 24 to 88 different initial configurations for each GB to improve the chances of locating the lowest-energy structures.

The misorientation range investigated is bounded by the $\Sigma=11/(113)$ ($\theta=50.48^\circ$) and $\Sigma=3/(111)$ ($\theta=109.47^\circ$) coherent twin GB's. Σ is defined as the ratio of the primitive unit-cell volume of the coincident-site lattice for the bicrystal to that of a single-crystal lattice. The structures of these GB's

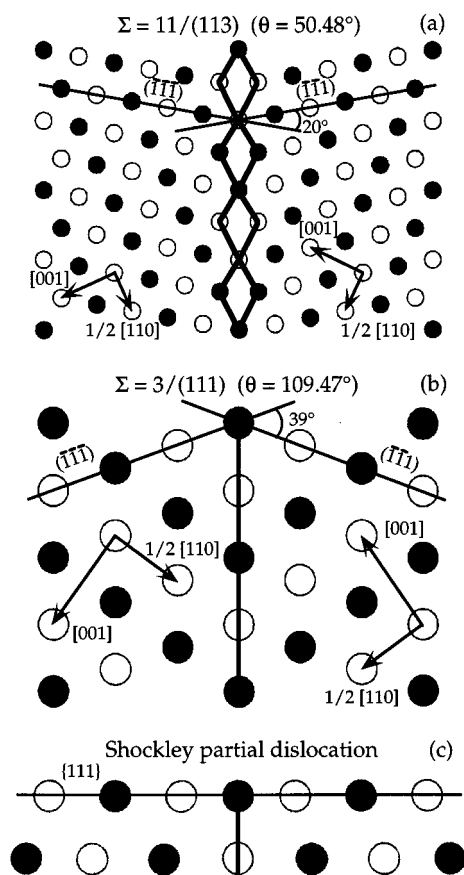


FIG. 1. Simulated structures of the (a) $\Sigma=11/(113)$ and (b) $\Sigma=3/(111)$ GB's in Ni. The structure of an isolated Shockley partial dislocation is shown in (c). The $[1\bar{1}0]$ tilt axis is perpendicular to the page and the atoms in the two $\{2\bar{2}0\}$ planes are shown as black or white. The $\Sigma=11/(113)$ and $\Sigma=3/(111)$ structural units and the location of the Shockley partial are indicated by bold lines. The bending of the $\{111\}$ planes as they cross the boundary is shown by the thin lines.

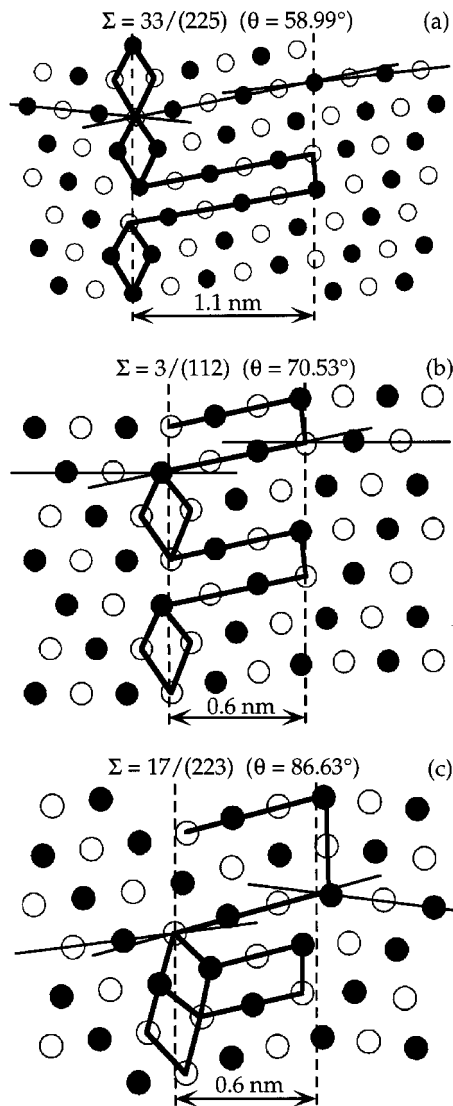


FIG. 2. The lowest energy structures simulated for the $\Sigma=33/(225)$ (a), $\Sigma=3/(112)$ (b), and $\Sigma=17/(223)$ (c) GB's in Ni. The GB's have dissociated into two boundaries indicated by dashed lines. The $\Sigma=11/(113)$ and $\Sigma=3/(111)$ structural units and the stacking faults between them are indicated by bold lines. The bending of the $\{111\}$ planes in the interboundary region is shown by the thin lines.

in Ni are exhibited in Fig. 1. The same structures are found for Al and Au. These are special boundaries that have GB energies much lower than neighboring boundaries.⁷ This is a result of the close-packed structural units (SU's) of these GB's. The quadrilateral SU's of the $\Sigma=11/(113)$ GB in Fig. 1(a) are capped-trigonal prisms, a random-close-packed structure.⁸ The $\Sigma=3/(111)$ SU's in Fig. 1(b) are indicated only by a vertical line since there is minimal distortion of the perfect crystal lattice on either side of the boundary. This SU is closely related to the Shockley partial dislocation that terminates an intrinsic stacking fault. The $\Sigma=3/(111)$ SU can be viewed as a Shockley partial in the edge orientation with a 39° bend in the $\{111\}$ planes that cross the boundary. The structure of an isolated Shockley partial⁹ is shown in Fig. 1(c).

The lowest-energy structures of three representative GB's

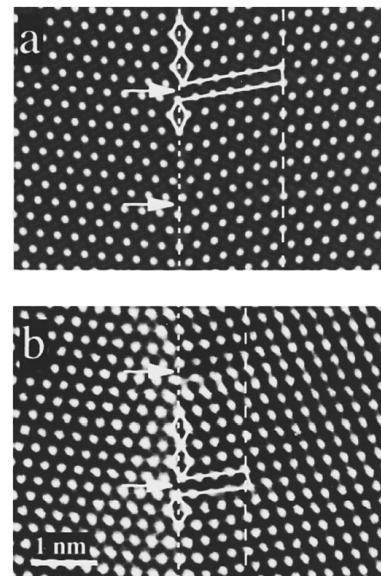


FIG. 3. The structure of the $\Sigma=33/(225)$ GB in Au. The main features in the simulated image from the computed Au structure (a) are in good qualitative agreement with the experimental HREM image (b). The locations of the stacking faults are shown by arrows and the dashed lines indicate the position of the boundaries.

in Ni with tilt angles between the two special GB's are shown in Fig. 2. In each case the GB has dissociated into two boundaries indicated by the dashed lines. The interboundary region is 0.6 to 1.1 nm wide. $\Sigma=11/(113)$ SU's are found on the left-hand boundary whereas vertical line segments, corresponding to the $\Sigma=3/(111)$ SU's, are found on the right-hand boundary. The $\Sigma=3/(111)$ SU's are at the end of intrinsic stacking faults in the interboundary region. In the $\Sigma=33/(225)$ ($\theta=58.99^\circ$) GB, stacking faults and $\Sigma=3/(111)$ SU's occur between every third $\Sigma=11/(113)$ SU. At larger tilt angles the ratio of $\Sigma=3/(111)$ to $\Sigma=11/(113)$ SU's increases. In the $\Sigma=3/(112)$ ($\theta=70.53^\circ$) GB the ratio is one to one. In the $\Sigma=17/(223)$ ($\theta=86.63^\circ$) GB there are three $\Sigma=3/(111)$ SU's for each $\Sigma=11/(113)$ SU. Since the $\Sigma=3/(111)$ SU's are not separate they do not all form stacking faults. Another SU appears in this GB above the $\Sigma=11/(113)$ SU that has the effect of shifting one of the $\Sigma=3/(111)$ SU's down by one $\{111\}$ plane. In addition to stacking faults, the $\{111\}$ planes in the interboundary region are also bent. As can be seen from the thin lines drawn along the $\{111\}$ planes in Fig. 2, they are bent upward at the $\Sigma=11/(113)$ SU's and downward at the $\Sigma=3/(111)$ SU's.

High-resolution electron microscopy (HREM) observations have recently been performed on Au bicrystals with $[1\bar{1}0]$ tilt GB's at misorientation angles between 50.5° and 59° .¹ The thin-film bicrystals were prepared by a modified Schober-Balluffi method.^{1,10} A JEOL 4000EX high-resolution electron microscope was employed for HREM observations, which were performed under axial illumination with the electron beam parallel to $[1\bar{1}0]$. Photographic images were recorded at focal settings near the optimum defocus. For comparison of the experimental observations to the computed Au structures the EMS suite of programs¹¹ was used to simulate HREM images using the multislice algorithm.

A simulated HREM image based on the calculated $\Sigma=33/(225)$ GB in Au is shown in Fig. 3(a). In this image, which was generated for a defocus of -55 nm and a thickness of 7.2 nm, the white dots closely correspond to the positions of the atomic columns. The lowest-energy computed Au structure that was used to form this image shows the same form of GB dissociation as the Ni structure in Fig. 2(a). The image contains two stacking faults located at the arrows. The $\Sigma=11/(113)$ SU's and stacking faults in one boundary period are outlined. The dashed lines indicate the locations of the two boundaries. The interboundary region is slightly wider than it is in the Ni structure [see Fig. 2(a)].

The HREM image in Fig. 3(b) shows good qualitative agreement with the corresponding calculated and simulated image in Fig. 3(a). The presence of stacking faults, the positions of which are indicated by arrows, is clearly seen when viewing the figure at a shallow angle along the (111) planes crossing the faults. The image contrast due to the stacking faults is somewhat more pronounced than in the simulated image. This may be due to surface strain effects that could cause local bending in the thin sections necessary for HREM. The dashed lines indicate the approximate positions of the two boundaries. The partial dislocations at the ends of the stacking faults show considerable delocalization, which makes it difficult to accurately determine the positions of the boundaries. The interboundary region is about two-thirds as wide as in the simulated image. This is expected since the EAM potential for Au has a stacking fault energy that is an order of magnitude lower than the experimental value. The effect of the stacking fault energy on this mode of GB relaxation is further discussed below.

This mode of GB relaxation can be understood if the boundaries are viewed as being vicinal to either the $\Sigma=11/(113)$ or $\Sigma=3/(111)$ singular GB's. Small misorientation deviations from a singular GB can be accommodated by an array of secondary grain-boundary dislocations (SGBD's). Deviations in the boundary plane orientation can be accommodated by steps in the boundary. In this way GB's that are vicinal to singular GB's can maintain the low-energy structure of the singular GB except for steps containing SGBD's. In the following discussion the vicinal $\Sigma=11/(113)$ description is used although the vicinal $\Sigma=3/(111)$ description is equally applicable. The misorientation of the $\Sigma=33/(225)$ GB is 8.51° from the $\Sigma=11/(113)$ misorientation. From a modified Read-Shockley-Frank formula,

$$|\mathbf{b}_{\text{SGBD}}| = 2D \sin\left(\frac{\Delta\theta}{2}\right), \quad (1)$$

where D is the distance between the SGBD's and $\Delta\theta$ is the misorientation deviation angle, the total Burgers vector of the SGBD's required is determined to be $\mathbf{b}_{\text{SGBD}} = \frac{2}{11}[113]$. The (225) average boundary plane can be arrived at by introducing steps in the (113) plane. This can be seen by looking at the periodic vector in a boundary plane perpendicular to the tilt axis. For the $\Sigma=33/(225)$ GB, the periodic vector is $\frac{1}{2}[554]$, which can be separated into units of the $\Sigma=11/(113)$ periodic vector and a step, $\frac{1}{2}[554] = \frac{3}{4}[332] + \frac{1}{4}[112]$. Thus, one period of the $\Sigma=33/(225)$ GB is comprised of one and a half periods of the $\Sigma=11/(113)$ GB and a step that is half a

period of the $\Sigma=3/(111)$ GB. If the cores of the SGBD's in the steps are highly localized at the boundary, the $\Sigma=11/(113)$ SU's above the step are compressed while those below are expanded. Since the $\Sigma=11/(113)$ SU's are geometrically ideal random-close-packed structures, any distortion would be energetically unfavorable. The distortion is reduced if the dislocation cores dissociate. A Shockley partial dislocation is emitted from the boundary, forming a stacking fault, while the remaining partial stays at the boundary plane. The row of Shockley partials creates a second boundary to one side of the original boundary. The bending of the $\{111\}$ planes in the interboundary region can be estimated from Eq. (1) using the Burgers vectors of the two partials.¹² This bending is energetically favorable since it increases the angle of the $\{111\}$ planes closer to the ideal 20° at the $\Sigma=11/(113)$ SU's and closer to the ideal 39° of the $\Sigma=3/(111)$ SU's at the Shockley partials (see Fig. 1). This analysis applies to all GB's in this range, even when the ratio of $\Sigma=3/(111)$ SU's to $\Sigma=11/(113)$ SU's is greater than 1, such as at the $\Sigma=17/(223)$ GB. However, using the vicinal $\Sigma=3/(111)$ description for such GB's is more physically intuitive.

Since this GB relaxation mechanism involves the creation of stacking faults, it is only expected to occur in materials with a low stacking fault energy γ_{SF} . This mode of relaxation is found in the computer simulations of Au and Ni but not in Al. The γ_{SF} of Au, Ni, and Al are found experimentally to be about 45 , 128 , and 166 mJ m^{-2} , respectively.¹³ With computer simulations it is important to consider the γ_{SF} of the potentials used and not just the experimental values. The EAM potentials for Au, Ni, and Al give γ_{SF} values of 4.7 , 14 , and 106 mJ m^{-2} , respectively. Even though the γ_{SF} of the potentials are lower than the experimental values, the simulations for Au and Al are at least in qualitative agreement with experimental observations. Grain-boundary dissociation is seen experimentally with HREM in several Au GB's (see Fig. 3 and Ref. 1). In an HREM study of the $\Sigma=3/(112)$ incoherent twin GB in Al (Ref. 14) GB dissociation was not observed. It is not known if this mode of GB relaxation occurs in real Ni. However, since the experimental value of γ_{SF} for Ni is nearly as high as Al and higher than the γ_{SF} value of the Al EAM potential, GB dissociation would appear to be unlikely. Thus, the simulations with the Ni EAM potential should be interpreted as describing a generic low γ_{SF} fcc metal. Although only a few pure metals have very low γ_{SF} it is generally lowered by alloying.¹³ Thus, this may be an important mode of GB relaxation in many engineering materials, such as austenitic stainless steels, for example.

The $\Sigma=3/(112)$ incoherent twin GB has also been studied with HREM in Ag (Ref. 15) and Cu.¹⁶ The experimental γ_{SF} values for Ag and Cu are 22 and 78 mJ m^{-2} , respectively.¹³ The observed structures are very similar to the simulated Ni structure in Fig. 2(b). In Refs. 15 and 16 it was proposed that a new GB phase had been observed. This phase—the $9R$ polytype—is the fcc structure with a stacking fault on every third $\{111\}$ plane. From the current study it is apparent that there is nothing unique about the $\Sigma=3/(112)$ incoherent twin and the $9R$ phase. A different polytype would be required for each GB in this misorientation range if this type of description were used. Hence, a description using the language of

dislocation theory, as presented here, is more general.

This research is supported by the U.S. Department of Energy, Basic Energy Sciences-Materials, Grants Nos. DE FG-0289ER45403/05 and W-31-109-ENG-38. J.D.R. acknowledges the support of the Computational Sciences Graduate

Fellowship program at Ames Laboratory, Ames, Iowa, and the National Energy Research Supercomputer Center for computer time. This work made use of the MRL Central Facilities, which are supported by the National Science Foundation, under Grant No. DMR-9120521.

K. L. Merkle, *J. Phys. (Paris)* **51**, C1-251 (1990); *Ultramicrosc.* **37**, 130 (1991); *J. Phys. Chem. Solids* **55**, 991 (1994).

¹H. Ichinose and Y. Ishida, *J. Phys. (Paris)* **46**, C4-39 (1985); H. Ichinose, Y. Ishida, N. Baba, and K. Kanaya, *Philos. Mag. A* **52**, 51 (1985).

²A. G. Crocker and B. A. Faridi, *Acta Metall.* **28**, 549 (1980).

³M. S. Daw and M. I. Baskes, *Phys. Rev. Lett.* **50**, 1285 (1983); *Phys. Rev. B* **29**, 6443 (1984).

⁴F. Ercolessi and J. B. Adams, *Europhys. Lett.* **26**, 583 (1994).

⁵S. M. Foiles, M. I. Baskes, and M. S. Daw, *Phys. Rev. B* **33**, 7983 (1986).

⁶D. Wolf, *Acta Metall. Mater.* **38**, 781 (1990).

⁷J. D. Bernal, *Nature* **185**, 68 (1960).

⁸For a more detailed description of Schockley partial dislocations see W. T. Read, *Dislocations in Crystals* (McGraw-Hill, New York, 1953), p. 96.

⁹T. Schober and R. W. Balluffi, *Philos. Mag.* **21**, 109 (1970); T. Y. Tan, J. C. M. Hwang, P. J. Goodhew, and R. W. Balluffi, *Thin*

Solid Films **33**, 1 (1976).

¹⁰P. Stadelmann, *Ultramicrosc.* **21**, 131 (1987).

¹¹Since the two boundaries are no longer symmetric this equation is not strictly valid but it provides a very close approximation. Also, the Burgers vector of the emitted partial may not be exactly $\frac{1}{6}[112]$, which would introduce a small additional error in the amount by which the {111} planes are bent.

¹²L. E. Murr, *Interfacial Phenomena in Metals and Alloys* (Addison-Wesley, Reading, MA, 1975), p. 145.

¹³D. L. Medlin *et al.*, in *Atomic-Scale Imaging of Surfaces and Interfaces*, edited by D. K. Biegelson, D. J. Smith, and D. S. Y. Tong, MRS Symposia Proceedings No. 295 (Materials Research Society, Pittsburgh, 1993), p. 91.

¹⁴F. Ernst *et al.*, *Phys. Rev. Lett.* **69**, 620 (1992); D. Hofmann and M. W. Finnis, *Acta Metall. Mater.* **42**, 3555 (1994).

¹⁵U. Wolf *et al.*, *Philos. Mag. A* **66**, 991 (1992); D. Hoffmann and F. Ernst, *Ultramicrosc.* **53**, 205 (1994).